Localized modes in random arrays of cylinders

C. Vanneste and P. Sebbah
Laboratoire de Physique de la Matière Condensée, CNRS UMR 6622, Université de Nice–Sophia Antipolis, Parc Valrose, 06108 Nice Cedex 02, France
(Received 3 August 2004; published 23 February 2005)

Anderson localization of classical waves in random arrays of dielectric cylinders is numerically investigated as a function of the distribution of their diameters. We show that using polydispersed resonant scatterers increases the localization length, while using identical resonant scatterers fosters Anderson localization. We discuss this collective process and link it to the effect of proximity resonances that has been studied in the case of a small number of resonant scatterers.

DOI: 10.1103/PhysRevE.71.026612 PACS number(s): 42.25.Dd, 72.15.Rn

I. INTRODUCTION

The search for Anderson localization of classical waves such as electromagnetic or sound waves is still an active field of investigation. While the phenomenon of wave localization is established on firm theoretical grounds, its experimental or numerical observation is difficult. Adjusting the physical parameters such as the index contrast, the filling fraction, and the size of the scattering particles is a main issue to observe Anderson localization in finite-size experimental or numerical systems. Because of competing or detrimental effects to localization, the rule of the game is to find a system with a localization length as small as possible. For instance, observation of localization requires the localization length ξ to be shorter than the absorption length l_a, a condition, which is difficult to meet in experimental systems [1,2]. In numerical works, the size of the system must be larger than ξ. This implies large systems and subsequently large amounts of computer memory and computing time. This is certainly true in two dimensions (2D) and even worse in 3D, especially in the vicinity of the localization transition where ξ diverges.

In order to decrease the value of ξ, several approaches have been proposed in the past. For instance, localization of classical waves is favored by introducing a small amount of disorder in a periodic system, thus leading to the creation of localized states inside and at the edges of the gap [3,4]. An alternative is resonant scattering. Resonant scattering, which is actively investigated by different groups whose goal is the reduction of the threshold of random lasers [5,6], has been first considered in several theoretical works [7–10]. Because the scattering cross section can be strongly enhanced at the resonance frequency ω_0 of a scatterer, significant reduction of ξ is expected to occur at the same frequency. Indeed, bands of localized waves at frequencies close to the resonance of an individual scatterer have been found numerically in random arrays of two-dimensional [11] or three-dimensional [12] pointlike dipoles. However, some authors report significant deviations from this reasonable expectation [13–16]. Though the regime of localization seems to have been reached in several experimental and numerical systems using resonant scatterers, the results indicate that localization is observed in the vicinity but off the resonance frequencies of individual scatterers. For instance, experimental localization of microwaves in a waveguide containing alumina spheres has been observed in a narrow frequency window not located at the first Mie resonance of spherical particles but above it [13]. In the same way, numerical investigations of acoustic waves in liquid media containing air-filled cylinders lead to the observation of localization not at the single cylinder resonance peak but at a frequency just above it [14]. Recently, frequency windows of localized modes in open random arrays of parallel cylinders have been found shifted from the Mie resonances of individual cylinders [15]. Even worse, localization has been predicted to be difficult to reach in systems with strong individual scattering efficiencies [16], when optical volumes of the scatterers start to overlap, thus reducing the efficiency of the collective cross section. Hence, it appears that our understanding of the interplay of resonant scattering and localization is not yet complete and the question of whether resonant scattering is helpful for observing localization is still open.

We have shed new light on this problem by considering an open random system of 2D circular particles (or parallel cylinders). Since the system is open, energy can escape through the boundaries, allowing us to discriminate in time between short- and long-lived modes. Numerical investigation of this disordered system when the cylinders have the same radius has revealed the existence of frequency windows of long-lived modes with quality factors as high as 10^4 [15]. The spatial extension of the modes was small enough for the leakage through the open boundaries to be small. Such modes were good approximations of localized modes characterized by a localization length smaller than the system size L.

The frequencies of those localized modes have been found markedly shifted from the Mie frequencies of a single cylinder. Thus, the role played by the Mie resonances in the existence of localization was questioned again. In order to elucidate this point, we describe in this work the consequences of introducing dispersion into the diameters of the cylinders. If the frequencies of the Mie resonances really control the frequencies of the localized modes, widening the distribution of the cylinder diameters should lead to the widening of the localization windows. This is indeed what we observe. When the dispersion of the diameters progressively increases, the localization windows are broadened until they overlap, thus disappearing. Also the mode lifetimes decrease to become significantly shorter than the lifetimes without

dispersion. This result confirms that the localization windows are controlled by the Mie resonances and indicates that the localization length increases with the width of the diameter distribution. Hence, introducing dispersion of the cylinder diameters is detrimental to localization, or, conversely, identical resonant scatters with well-defined values of the resonance frequencies foster localization.

The paper is organized as follows. In Sec. II, we describe the physical and numerical parameters of the system of random circular particles. In Sec. III, we present and discuss the numerical results. The emergence of frequency bands of long-lived modes in random systems of identical cylinders is described first. Next, we describe the effect of enlarging the distribution of the diameters of the cylinders. Discussion of the results and conclusion are presented in Sec. IV. In particular, we link our results to the effect of proximity resonances that has been studied in the case of a small number of resonant scatterers [17,18].

II. DESCRIPTION OF THE SYSTEM

The system is very close to the one described in [15]. This is a 2D open random medium of size L^2, which consists of circular particles with diameter D and optical index n_2. The particles are randomly distributed in a background medium of optical index n_1. This system is equivalent to a random collection of cylinders oriented along the z axis. The filling fraction of the particles is $\Phi=40\%$. This value has been arbitrarily chosen in the range where localized modes were observed in [15]. The difference with [15] is that the diameters of the cylinders are not bound to be identical. They are randomly distributed in an interval $[D_{\min}, D_{\max}]$ centered at the value D_c. The distribution is uniform, its width being characterized by $\delta D=|D_{\max}-D_{\min}|$. The value of D_c has been chosen equal to 180 nm. Systems with different widths of the distribution have been studied, δD varying from 0 to 160 nm. For each value of the width, 15 different random systems have been investigated.

The electromagnetic field that propagates in the system has been chosen to be a 2D transverse magnetic (TM) field, so that Maxwell's equations read

$$\mu_0 \partial H_x/\partial t = -\partial E_z/\partial y,$$

$$\mu_0 \partial H_y/\partial t = \partial E_z/\partial x,$$

$$\varepsilon_i \varepsilon_0 \partial E_z/\partial t = \partial H_y/\partial x - \partial H_x/\partial y,$$

$$\varepsilon_i = n_i^2, \quad i=1,2,$$

where ε_0 and μ_0 are the electric permittivity and the magnetic permeability of vacuum, respectively.

The finite-difference time-domain (FDTD) method [19] has been used to solve Maxwell's equations. To model an open system, PML (perfectly matched layer) absorbing conditions [20] have been imposed at the boundaries of the system. The values of the space and time increments are $\Delta x=10$ nm and $\Delta t=\Delta x/c\sqrt{2}\approx 2.8\times 10^{-17}$ s, where c is the velocity of light in vacuum. Those values guarantee the stability of the FDTD algorithm. They are sufficiently small compared to the optical wavelengths $150\ \text{nm}\leqslant\lambda\leqslant 600$ nm and to the optical periods $5\times 10^{-16}\leqslant T\leqslant 2\times 10^{-15}$ s considered in the following to avoid significant numerical dispersion. In order to approach the localized regime, a large optical index contrast has been chosen between the particles and the background, namely $n_1=1$ and $n_2=2$. The total size of the system has been chosen equal to $510\times\Delta x$, which corresponds to $L\approx 5\ \mu$m.

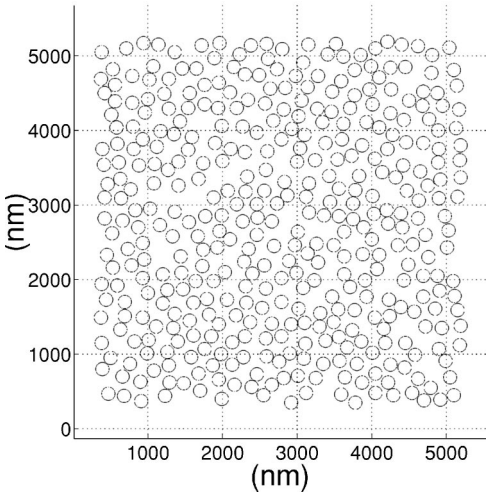

FIG. 1. An example of random realization of circular particles: $L=5\ \mu$m, $D=180$ nm, and $\Phi=40\%$.

To study the modes of the system, a short Gaussian electromagnetic pulse of duration about 10 time steps Δt is launched inside the system. The impulse response is recorded at several nodes regularly positioned in the system. The recorded fields are then added to obtain a signal averaged over the whole system. This procedure has been used to improve the detection of all the modes, including those which are strongly localized in a fraction of the system. When necessary, a monochromatic source at an eigenfrequency selected in the power spectrum is used in order to excite the corresponding eigenmode alone.

III. RESULTS

A. Identical cylinders

We review the case of random systems with identical cylinders. Those results have been partially presented in [15] and are extended here to a larger range of the spectrum that includes several frequency windows of long-lived modes.

1. Spectrum and nature of the modes

An example of a random array of identical cylinders with $\Phi=40\%$, $D=180$ nm, and $\delta D=0$ is displayed in Fig. 1. Let us consider the impulse response of this system in the time window $[t_1,t_2]$, where $t_1=T_w$ and $t_2=t_1+T_w$ (inset of Fig. 2). The corresponding power spectrum obtained by the Fourier transform of the signal averaged over several locations in the system is shown in Fig. 2 (note the vertical logarithmic scale). One observes that the peaks, which correspond to

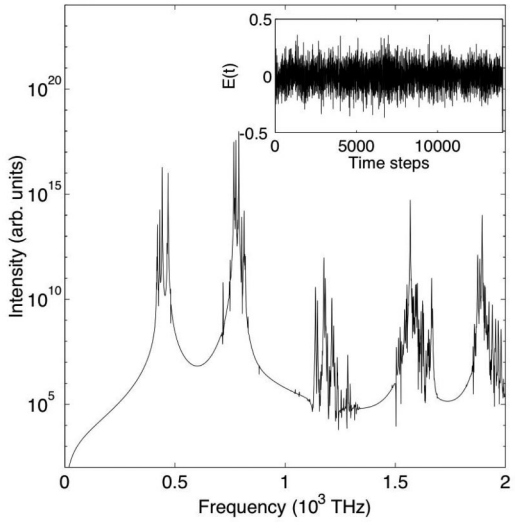

FIG. 2. Power spectrum of the impulse response of the system displayed in Fig. 1. Note the logarithmic vertical scale. The inset shows the impulse response recorded at some location inside the system in the time window $[T_w, 2T_w]$, where $T_w = 131072\ \Delta t \approx 3.7$ ps.

modes of the system, are grouped in distinct frequency windows. The same spectral structure has been observed for 15 different sample realizations. If the frequencies of individual peaks do depend on the realization of the disorder, the frequency windows do not. They only depend on the pair (D, Φ) [15]. The averaged spectrum over the 15 spectra corresponding to the same pair ($D = 180$ nm, $\Phi = 40\%$) is represented in Fig. 3. This demonstrates that the frequency windows cover the same frequency ranges as those shown in Fig. 2 for a single system.

In order to compare the positions of the above frequency windows with the frequencies of the Mie resonances of a

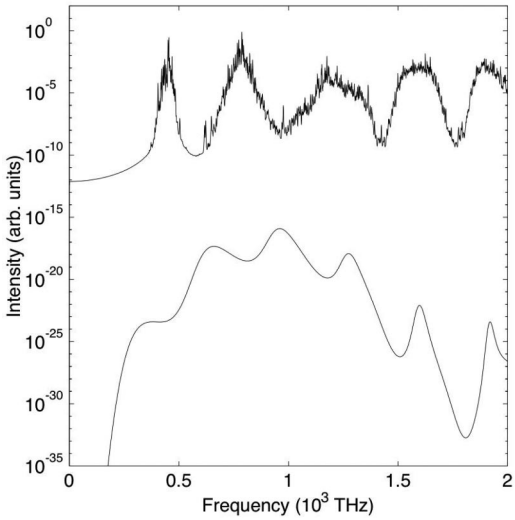

FIG. 3. Average of power spectra similar to Fig. 2 performed over 15 different random systems of cylinders. The bottom curve is the Mie scattering cross section of a TM wave incident upon a cylinder with index contrast $m = n_2/n_1 = 2$. For clarity, the different curves have been shifted vertically.

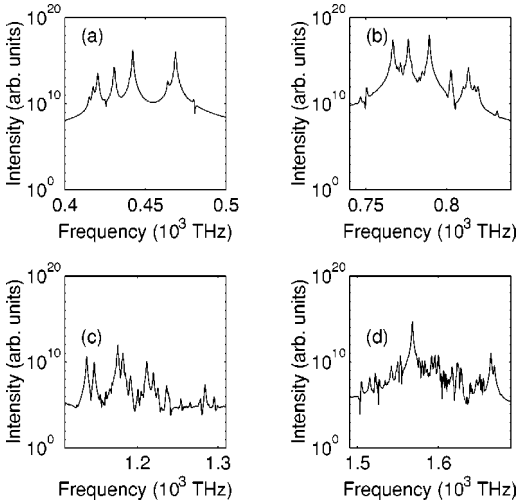

FIG. 4. Enlargements of the four first frequency windows of the spectrum shown in Fig. 2.

single cylinder, the scattering cross section of a TM wave incident on a cylinder of index $n_2 = 2$ embedded in a medium of index $n_1 = 1$ has also been shown in Fig. 3. One observes that the frequency windows are shifted from the Mie resonances. Hence, the resonances of the random system of cylinders do not coincide with the maxima of the scattering cross section of the individual scatterers as opposed to what one might first expect. This observation is in agreement with the observation of localization of microwaves [13] and acoustic waves [14] in narrow frequency ranges away from the Mie resonances.

Figure 4 displays enlargements of the four first frequency windows in Fig. 2. It can be seen that well-separated peaks can be identified in the low-frequency windows [Figs. 4(a) and 4(b)]. In the higher-frequency windows [Figs. 4(c) and 4(d)], the density of states is larger as expected and peaks start to overlap significantly. We shall see in Sec. III A 2 that the two low-frequency windows and the two high-frequency windows correspond to long- and short-lived modes, respectively.

In order to study the nature of the modes corresponding to individual peaks, a monochromatic source is used to excite each of them separately. To excite a given mode, the frequency of the source is adjusted at the value of the corresponding peak measured in the spectrum. For the two low-frequency windows, the monochromatic source has a Gaussian envelope of duration larger than the inverse of the level spacing between two neighbor modes such that each mode is excited alone. Figure 5 shows spatial maps of such excited eigenmodes at the end of the emission of the monochromatic source. These modes display a strong spatial localization. As in [15], we have observed an exponential decay of their envelope. The average decay lengths, which can be identified to the localization length ξ, have been measured to be $\xi \approx 0.4\ \mu$m for the first low-frequency window and $\xi \approx 0.42\ \mu$m for the second one. These values are significantly smaller than the size $L \approx 5\ \mu$m of the system.

Excitation of the modes belonging to the high-frequency windows is slightly different. Since such modes have a very

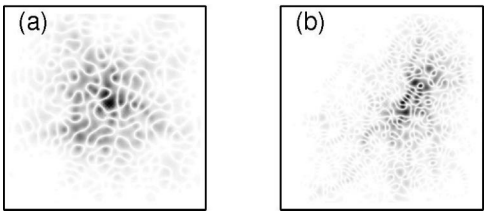

FIG. 5. Spatial maps of excited eigenmodes at the end of the emission of the monochromatic source (a) fourth peak from the left of the frequency window displayed in Fig. 4(a), (b) first peak from the left of the frequency window displayed in Fig. 4(b).

short lifetime, they decay and merge into the background radiation before the source is completely extinguished at the end of the Gaussian envelope. Hence, it is not possible to observe them after the end of the emission of the source, contrary to the modes of the low-frequency windows. Therefore, after a smooth build-up transient, the amplitude of the monochromatic source has been maintained at a steady value. Hence, the resulting spatial maps as shown in Fig. 6 represent the Green function of the system in the frequency domain. They correspond to system resonances, which are mixed to some non-negligible extent with their neighbors, rather than single modes as in Fig. 5. Although, they are reasonably well centered inside the system, their spreading is larger than the modes of the low-frequency windows. The average decay lengths have been measured to be $\xi \approx 0.6\ \mu$m for the third window and $\xi \approx 0.65\ \mu$m for the fourth. Thus, such modes have a decay length ξ larger than those in Fig. 5. Though ξ is still smaller than the size of the system, those modes are not well localized. For a mode well centered in the system, the ratio of the field amplitude at the boundaries over the maximum amplitude at the center is estimated to be $e^{-L/4\xi}$. When ξ varies from $\xi \approx 0.4\ \mu$m to $\xi \approx 0.65\ \mu$m, this ratio varies from 0.044 to 0.15 for $L = 5\ \mu$m. Thus, for $\xi \approx 0.65\ \mu$m, the amplitude of the field at the boundaries is not negligible. This leads to significant energy leakage of the modes [21] and a short lifetime, as shown in the next section. Moreover, the value of the measured decay length in the high-frequency windows increases when one enlarges the system by adding external layers of cylinders as discussed in Sec. III A 3. Hence, the measured decay length is not an intrinsic property of the resonance but depends on the size of the system. By contrast, the resonance decay lengths in the low-frequency windows do not depend on the size L of the system.

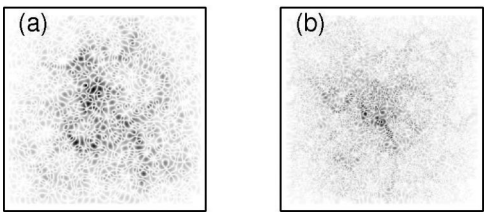

FIG. 6. Spatial maps obtained when the amplitude of a monochromatic source is maintained at a steady value for resonances of the third and fourth frequency windows (a) third peak from the left of the frequency window displayed in Fig. 4(c), (b) largest peak of the frequency window displayed in Fig. 4(d).

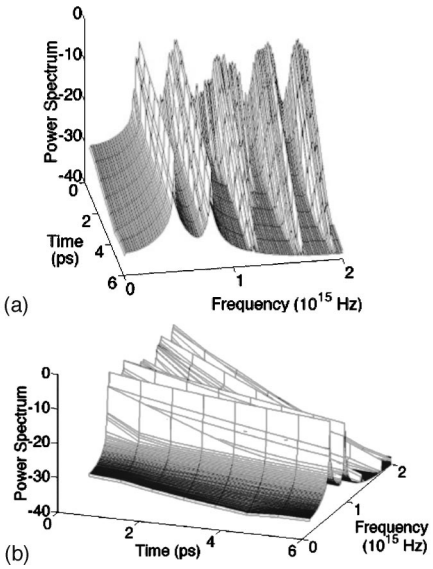

FIG. 7. Evolution of the power spectrum averaged over 15 different systems of identical cylinders as a function of time.

2. Time evolution of the spectrum

Since the energy of the pulse progressively leaves the system through the open boundaries of the system according to the different decay times of the excited modes, the recorded field is not stationary and the power spectrum evolves with time. To follow this time evolution, the signal is Fourier-transformed in several successive time windows of length $T_w = 131\,072\ \Delta t \approx 3.7$ ps. The time delay between successive windows has been chosen equal to $T_d = 32\,768\ \Delta t \approx 0.9$ ps so that there is a strong overlap between successive windows. We thus obtain a rather smooth evolution with time of the power spectrum of the system.

The evolution of the power spectrum as a function of time is displayed in Fig. 7. As in Fig. 3, the spectrum is the average over the disorder of 15 different spectra. Thus, we can focus our attention over the general evolution of the frequency windows rather than the behavior of individual peaks. In order to obtain a better view of the evolution of the spectrum, the same three-dimensional representation has been displayed under two different orientations in Figs. 7(a) and 7(b), respectively. In Fig. 7(a), the different frequency windows are manifest. The most noticeable feature of the figure is the regular decay with time of the power spectrum regardless of the frequency. This behavior is expected since the energy escapes the system through the open boundaries. However, Fig. 7(b) shows that the decay time τ depends strongly on the frequency. It is clear that it is much longer for the two low-frequency windows than for the other high-frequency windows. The values of the longest decay times in the two low-frequency windows have been measured to be 1.1 ps and 1.0 ps, respectively. In the high-frequency windows, the decay time barely depends on the frequency. Its maximum value is 0.2 ps.

3. Effect of the system size

Recapitulating the preceding results, random systems of identical parallel cylinders exhibit resonances, which are

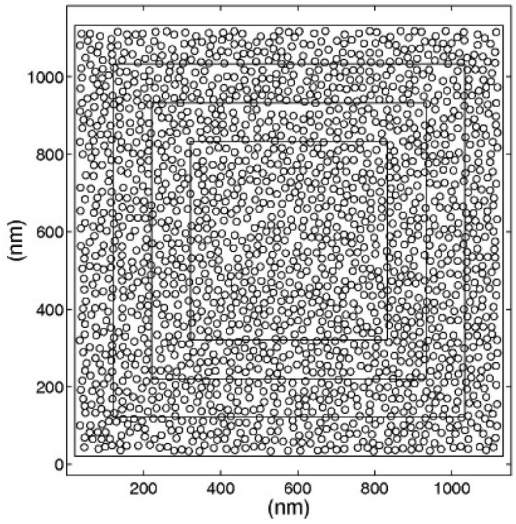

FIG. 8. New systems obtained after adding one after the other three external layers of cylinders to the system in Fig. 1. The frames indicate the external boundaries of each system. Note that the system inside the smallest frame is identical to the system in Fig. 1.

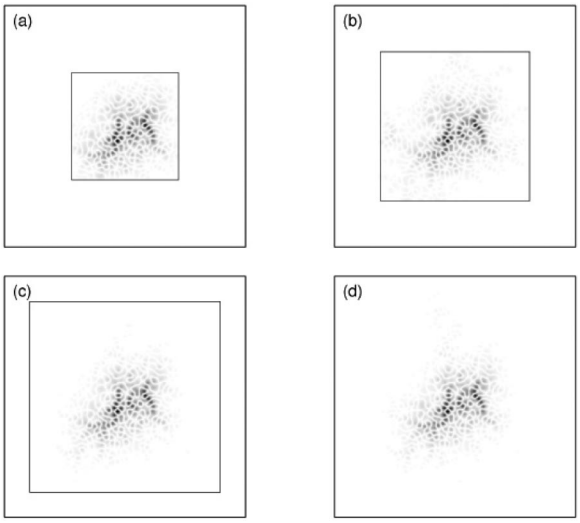

FIG. 9. Spatial maps of a resonance belonging to the first low-frequency window for the four systems shown in Fig. 8. The frames indicate the (open) boundaries of each system as in Fig. 8.

grouped in separate frequency windows. In the low-frequency windows, these resonances correspond to long-lived modes, which can be considered as localized modes characterized by a localization length ξ significantly smaller than the size L of the system. In high-frequency windows, the resonances exhibit more extended spatial maps which lead to significant leakage and short mode decay times. Why did we find two and not one or three windows of well localized modes? A reasonable explanation is that this is due to the choice of the size L of our system. More precisely, the number of windows of localized modes is determined by the ratio L/D. Using larger systems would lead to the progressive evolution of frequency windows of short-lived resonances into frequency windows of localized modes when the size L is sufficiently larger than the corresponding localization length ξ.

In order to illustrate the importance of the ratio L/D, we have increased the size of some samples from $L=5$ μm to $L=11$ μm by adding successive external layers of cylinders whose thickness is 1 μm (Fig. 8). The maps of a mode belonging to the first low-frequency window when $L=5$ μm, $L=7$ μm, $L=9$ μm, and $L=11$ μm are compared in Figs. 9(a)–9(d). As expected, the external layer of cylinders does not perturb this mode, which was already well localized in the box $L=5$ μm. In particular, its decay length is the same for all values of L. However, its decay time has been measured as increasing from 1 ps to 212 ps when L has increased from 5 to 11μm. For comparison, the maps of a resonance belonging to the third frequency window when L increases from 5 to 11μm are shown in Figs. 10(a)–10(d). One observes that the patterns are significantly perturbed by the addition of external layers. The decay length has been measured to increase from Fig. 10(a) to Fig. 10(d), meaning that its value is controlled by the size of the system. The fact that the additional layer of scatterers modifies the spatial map of the resonance demonstrates that localization has not been reached yet. Moreover, the decay time of the resonance in the enlarged systems has been measured to stay smaller than 0.2 ps, indicating again that the localization length is still too large at the frequency of the mode.

As a final point, these results show that the localization length in random systems of parallel cylinders significantly depends on the frequency. Actually, previous theoretical results [7,8] have concluded that there is a multitude of mobility edges and localization regions in such systems with a general trend for ξ to increase with frequency. Our numerical results are in good agreement with those theoretical results, which predict the shortest values of ξ at low frequencies.

B. Nonidentical cylinders

We consider now the case of nonidentical cylinders. Not only are the positions of the cylinders random as in the pre-

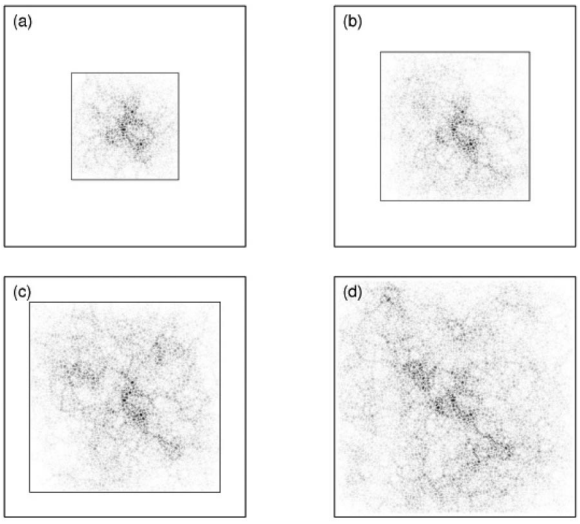

FIG. 10. Spatial maps of a resonance belonging to the third frequency window for the four systems shown in Fig. 8. The frames indicate the (open) boundaries of each system as in Fig. 8.

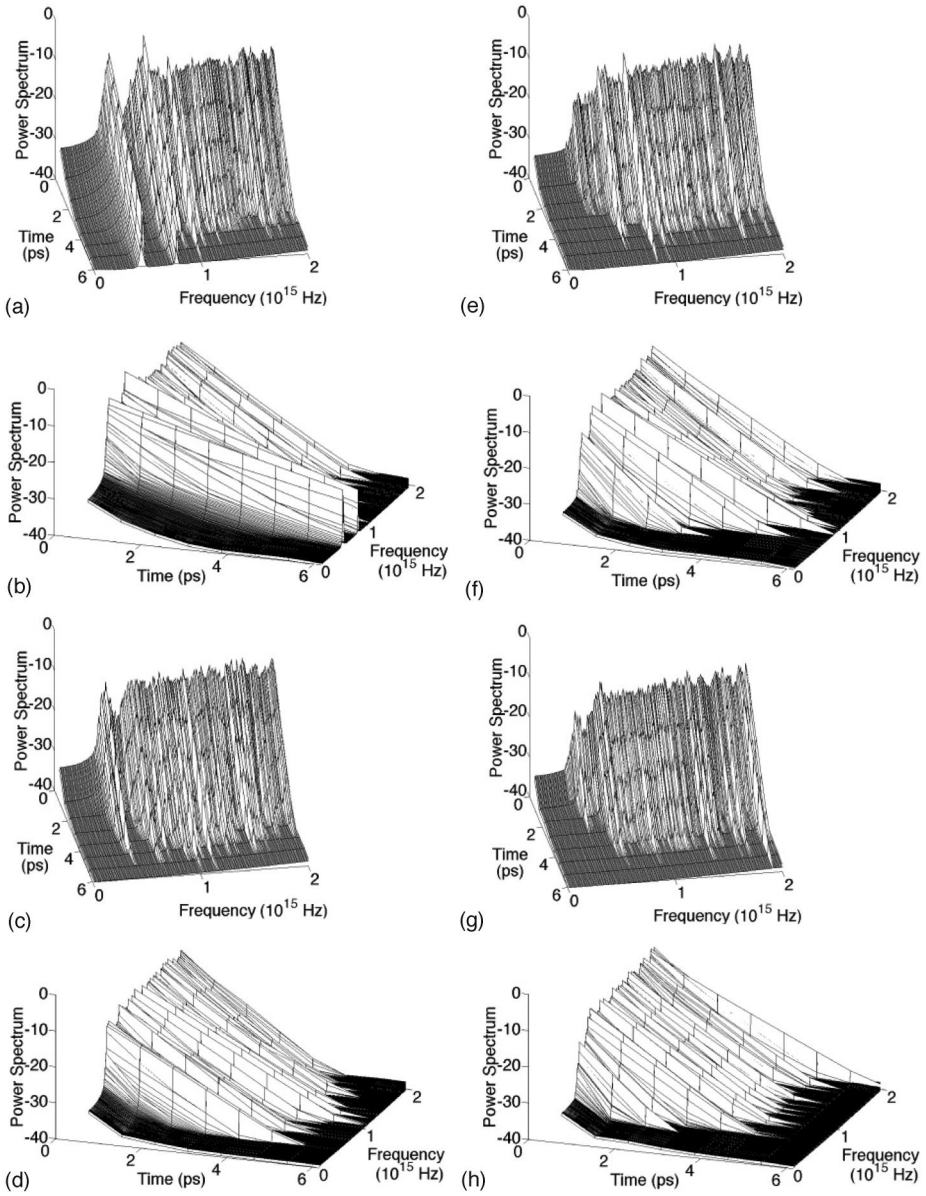

FIG. 11. Evolution of the power spectrum averaged over 15 different systems as a function of time for increasing values of the width δD of the diameter distribution of the cylinders (a) and (b) $\delta D = 40$ nm, (c) and (d) $\delta D = 80$ nm, (e) and (f) $\delta D = 120$ nm, and (g) and (h) $\delta D = 160$ nm. The average diameter is $D_c = 180$ nm.

ceding section, but their diameters are randomly distributed over the interval $[D_{\min}, D_{\max}]$ centered at the value $D_c = 180$ nm. The distribution is uniform and its width is characterized by $\delta D = |D_{\max} - D_{\min}|$. Four different widths have been considered ($\delta D = 40$, 80, 120, and 160 nm) and compared with the case $\delta D = 0$ of identical cylinders investigated in Sec. III A.

The evolution of the power spectra as a function of time is shown in Fig. 11. As previously, 15 different realizations of the disorder have been studied for each of the five values of δD. The spectra displayed in Fig. 11 are averages over the corresponding individual spectra. Again, the three-dimensional representations have been displayed under two different orientations in order to show various features of the spectra.

Let us compare the case $\delta D = 40$ nm in Figs. 11(a) and 11(b) with the case $\delta D = 0$ in Figs. 7(a) and 7(b). Two main differences can be observed. First, Fig. 10(a) shows that the high-frequency windows have disappeared. They are replaced by an almost uniform spectrum without "gaps." In contrast, the two low-frequency windows are still well distinct. The second difference is the increase of the decay rates at all frequencies. Compared with the case of identical cylinders, the longest decay times have shortened from 1.1 and 1.0 ps to 0.39 and 0.27 ps for the two low-frequency windows and from 0.2 to 0.15 ps for the high-frequency windows. This behavior is confirmed when the distribution width is increased to $\delta D = 80$ nm [Figs. 11(c) and 11(d)]. The second low-frequency window has now merged into the higher frequency range of the spectrum. Only the first low-frequency window is still distinct. Moreover, the decay time has become quite uniform over the whole frequency range. Its maximum value is 0.17 ps. By increasing again δD to 120 nm [Figs. 11(e) and 11(f)] and next to 160 nm [Figs. 11(g) and 11(h)], the spectra and the decay times stay uniform. The decay times are slightly shorter than for $\delta r = 80$ nm with the same maximum value about 0.17 ps. The first low-frequency window is still just discernible with decay times surprisingly

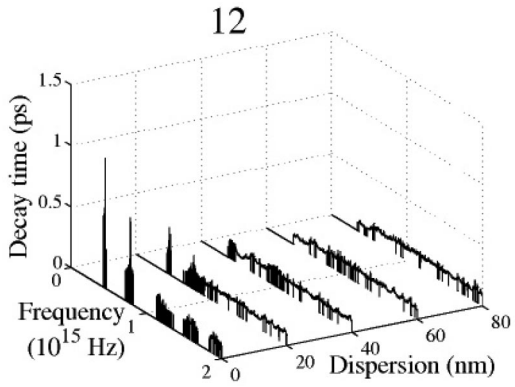

FIG. 12. Decay times of the resonances as a function of the frequency for increasing values of the width δD of the diameter distribution of the cylinders.

shorter (less than 0.1 ps) than the average decay time at other frequencies.

These results are recapitulated in Fig. 12, which displays the decay times as a function of frequency for increasing values of the distribution width. The limited amount of sample realizations is nonetheless sufficient to display the general trend just discussed. The peaks of decay times corresponding to the initial frequency windows at zero dispersion merge into a flat plateau when the width of the diameter distribution increases.

IV. DISCUSSION AND CONCLUSION

In conclusion, we have demonstrated the existence of frequency bands of long-lived modes in random systems of identical cylinders, which confirm the preliminary results presented in [15]. Such modes are sufficiently well localized inside the finite system that we have considered for the leakage through the open boundaries to be small. They can be considered as good approximations of localized modes characterized by a localization length smaller than the system size L. The frequencies of these modes are significantly shifted from the Mie frequencies of the cylinders, thus questioning the role played by internal resonances in Anderson localization. Next, we have considered nonidentical cylinders with different diameters in order to mix different resonance frequencies of the scatterers. We have found that the well-localized modes observed when the cylinders are identical evolve into short-lived resonances. This result indicates that the localization length has increased up to values such that the field at the boundaries of the system is no longer negligible. This strongly suggests that the Mie resonances control the frequencies of the localized modes that are observed with identical cylinders.

Then, the question is why are the frequencies of the localized modes shifted from the Mie frequencies where the scattering efficiency is maximum? As a matter of fact, such a shift is expected. Mie frequencies are characteristic of isolated scatterers. Whenever, a collection of scatterers is considered, they cannot be regarded as independent except at very low density. This is comparable to the interaction of atoms in a solid. In particular, if the atoms are identical, the level degeneracy will be destroyed by any interaction, thus leading to the appearance of new frequencies in the spectrum of the system. In the same way, the resonances of a collection of scatterers differ from the resonances of isolated scatterers. This effect has been recently investigated for a collection of few scatterers [17,18] and has been called proximity resonance. In that case, it was shown that the resonances of individual scatterers were modified into large and also very narrow resonances. Similar results about the scattering cross section of one, two, and three cylinders with gain have been recently obtained in the search of high-Q cavities in random lasers [5]. We believe that the long-lived modes that are observed in random system of identical cylinders correspond to the manifestation of the proximity resonance effect when the collection of scatterers is large.

The results presented in this paper concern systems of cylinders that have a higher optical index than the background medium. The present knowledge for inverted media is not clear. For instance, scattering has been reported to be less efficient for cylinders that have a smaller dielectric constant than the background medium [7]. Hence, particle resonances are expected to play a smaller role. However, in contrast with this result, the mean free path in systems of spherical holes randomly distributed in, e.g., silicon is known to be smaller than for spheres of silicon in air [22]. Therefore, extending this investigation to such inverted media would be helpful for clarifying this point. The answer should have an impact in experiments devoted to lowering the threshold of random lasers. It would also be highly valuable to extend this investigation to systems of spherical scatterers such as those which have been experimentally investigated in [6,13]. It is likely that the present conclusions are also valid for the 3D case.

[1] A. Z. Genack and N. Garcia, Phys. Rev. Lett. **66**, 2064 (1991).
[2] D. S. Wiersma, P. Bartolini, A. Lagendijk and R. Righini, Nature (London) **390**, 671 (1997); F. Scheffold, R. Lenke, R. Tweer, and Georg Maret, *ibid.* **398**, 206 (1999); D. S. Wiersma, G. S. Rivas, P. Bartolini, A. Lagendijk, and R. Righini, *ibid.* **398**, 207 (1999).
[3] S. John, Phys. Rev. Lett. **58**, 2486 (1987).
[4] M. M. Sigalas, C. M. Soukoulis, C.-T. Chan, and D. Turner, Phys. Rev. B **53**, 8340 (1996).
[5] J. Ripoll, C. M. Soukoulis, and E. N. Economou, J. Opt. Soc. Am. B **21**, 141 (2004).
[6] X. H. Wu, A. Yamilov, H. Noh, H. Cao, E. E. Seelig, and R. P. H. Chang, J. Opt. Soc. Am. B **21**, 159 (2004).
[7] P. Sheng and Z. Q. Zhang, Phys. Rev. Lett. **57**, 1879 (1986).
[8] C. A. Condat and T. R. Kirkpatrick, Phys. Rev. B **36**, 6782 (1987).

[9] D. Sornette and B. Souillard, Europhys. Lett. **7**, 269 (1988).
[10] For a discussion of resonant scattering, see A. Lagendijk and B. A. van Tiggelen, Phys. Rep. **270**, 143 (1996).
[11] M. Rusek, A. Orlowski, and J. Mostowski, Phys. Rev. E **56**, 4892 (1997).
[12] M. Rusek, J. Mostowski, and A. Orlowski, Phys. Rev. A **61**, 022704 (2000).
[13] A. A. Chabanov and A. Z. Genack, Phys. Rev. Lett. **87**, 153901 (2001).
[14] E. Hoskinson and Z. Ye, Phys. Rev. Lett. **83**, 2734 (1999).
[15] P. Sebbah and C. Vanneste, Phys. Rev. B **66**, 144202 (2002).
[16] B. A. van Tiggelen, A. Lagendijk, A. Tip, and G. F. Reiter, Europhys. Lett. **15**, 535 (1991).
[17] E. J. Heller, Phys. Rev. Lett. **77**, 4122 (1996).
[18] Sheng Li and E. J. Heller, Phys. Rev. A **67**, 032712 (2003).
[19] A. Taflove, *Computational Electrodynamics: The Finite-Difference Time-Domain Method* (Artech House, Norwood, 1995).
[20] J. P. Berenger, J. Comput. Phys. **114**, 185 (1995).
[21] F. A. Pinheiro, M. Rusek, A. Orlowski, and B. A. Van Tiggelen, Phys. Rev. E **69**, 026605 (2004).
[22] D. Wiersma (private communication).